Electronic Supplementary Material (ESI) for Dalton Transactions.
This journal is © The Royal Society of Chemistry 2023

Supporting Information

One-step synthesis of 2D@3D hollow prussian blue analogue as high-performance bifunctional electrochemical sensor

Tian Liu [a], Jiang Wang [a], Qiao Jiang [a], Ning Chai [a], Shuanglu Ying [a], Yuxuan Kong [a], and Fei-Yan Yi [a, b, *]

[a] School of Materials Science and Chemical Engineering, Ningbo University, Ningbo, Zhejiang, 315211, P. R. China, E-mail: yifeiyan@nbu.edu.cn

[b] Key Laboratory of Photoelectric Detection Materials and Devices of Zhejiang Province, Ningbo, 315211, P. R. China.

Experimental Section

Materials. Cobalt nitrate hexahydrate ($Co(NO_3)_2·6H_2O$), Anhydrous dextrose, Disodium hydrogen phosphate dodecahydrate ($Na_2HPO_4·12H_2O$), Potassium chloride (KCl), Magnesium sulfate heptahydrate ($MgSO_4·7H_2O$), Ammonium chloride (NH_4Cl), Sodium sulfate ($NaSO_4$), Calcium chloride ($CaCl_2$), Sodium acetate anhydrous (NaAC), Aodium citrate ($C_6H_5Na_3O_7·2H_2O$), Potassium ferricyanide ($K_3[Fe(CN)_6]$) and Sodium chloride (NaCl) were purchased from Sinopharma chemical reagent Co., Ltd. Dopamine hydrochloride (DA) was supplied by Shanghai Macklin Biochemical Co., Ltd. Goat serum, Ascorbic acid (AA) and Uric acid (UA) were acquired from Shanghai yuanye Bio-Technology Co., Ltd. Sodium nitroprusside ($Na_2[Fe(CN)_5(NO)]·2H_2O$) and L-(+)-Lactic acid (LA) were acquired from Rhawn. Sodium nitrite ($NaNO_2$) and Sodium dihydrogen phosphate dihydrate ($NaH_2PO_4·12H_2O$) were obtained from Macklin. All chemicals in the experiment were directly used without any purification.

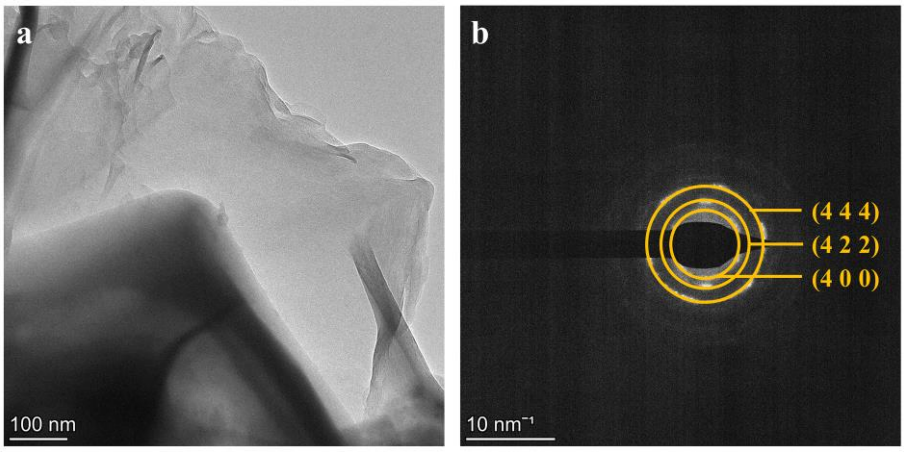

Fig. S1 (a) TEM image of HTPBA-12 and (b) corresponding SAED pattern.

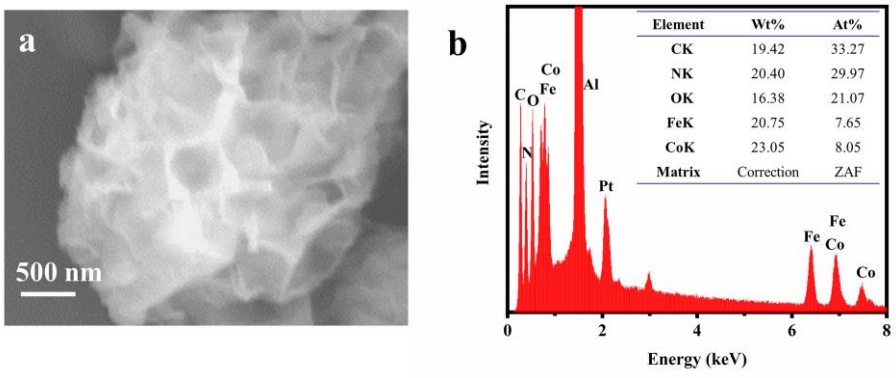

Fig. S2 (a) SEM image of HTPBA-12 and (b) corresponding EDS spectrum (inset: The obtained elemental ratio).

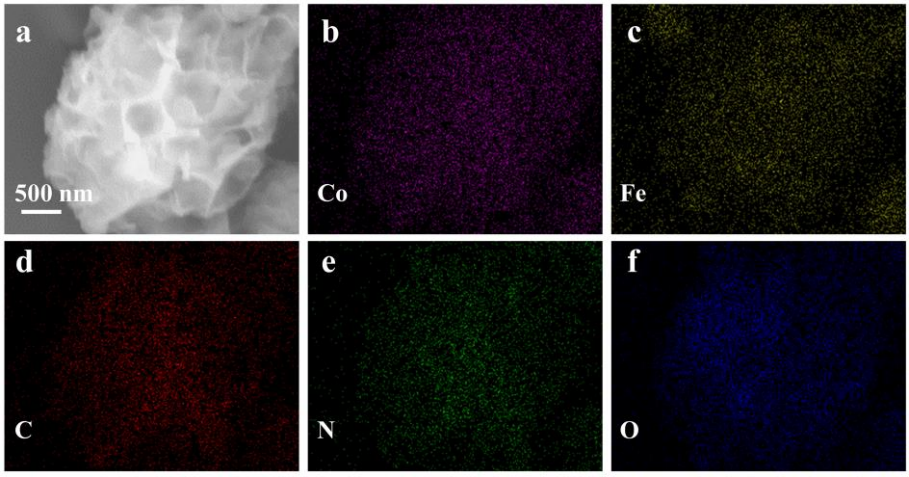

Fig. S3 (a) SEM image of HTPBA-12 and (b-f) corresponding elemental mapping.

Table S1. ICP-OES results of HTPBA-12.

Element	Wt%	Atomic%
Na	0.00513	0.000223
Co	9.38	0.159
Fe	9.31	0.167

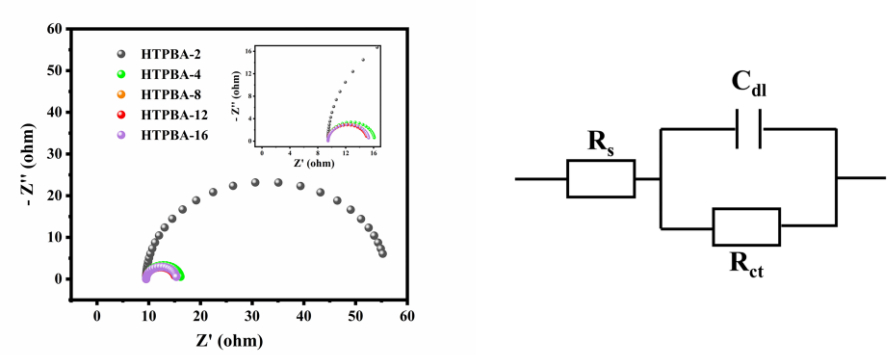

Fig. S4 The EIS curves of HTPBA/NF and the equivalent circuit.

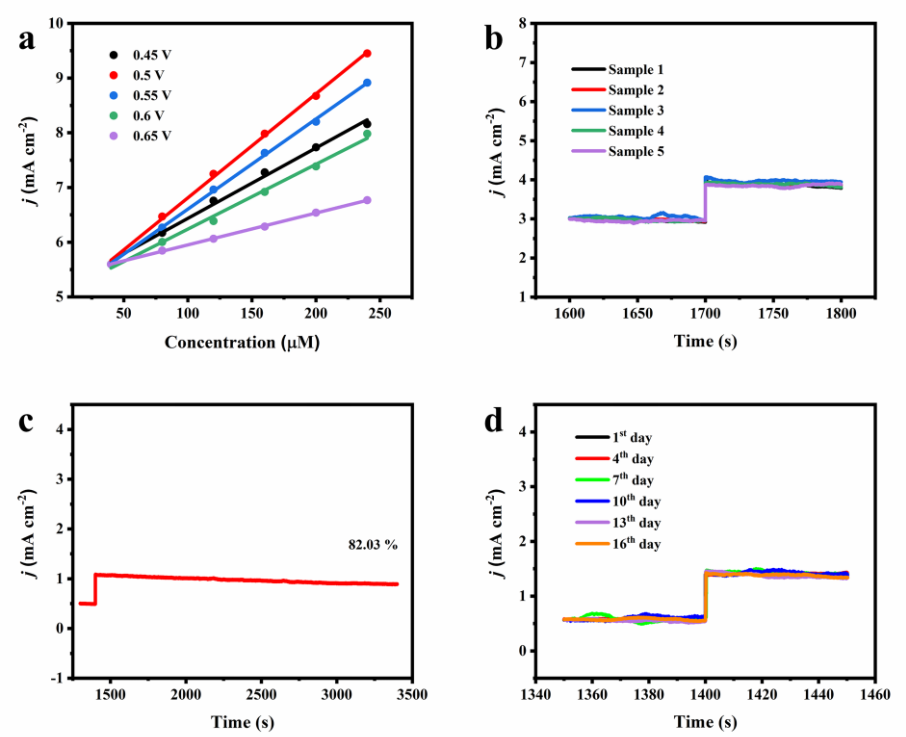

Fig. S5 (a) Dependence of amperometric response at HTPBA/NF-12 on applied potential; (b) Amperometric responses of five identical HTPBA/NF-12 electrodes to 50 μM glucose in 0.1 M NaOH; Amperometric response of the HTPBA/NF-12 electrode (c) to 20 μM glucose in 0.1 M NaOH for a long running time and (d) measured by injecting 30 μM glucose into 0.1 M NaOH every 3 days over 16 days.

Table S2. Comparison of HTPBA/NF-12 with other related materials for glucose detection.

Electrode	Sensitivity, ($\mu A\ mM^{-1}\ cm^{-2}$)	Linear Range, (μM)	LOD, (μM)	Working potential, (V)	Electrolyte	Ref.
CoFePBA/FTO	18.69	100~8200	67	1.15 (vs Ag/AgCl)	0.1 M PBS	5
Au@NiFePBA/Nafion	8.037	10~16000	4.686	0.22 (vs Ag/AgCl)	0.1 M NaOH	21
NiFePBA/NF	21040, 6570	2~263.3,263.3~650	0.2	0.5 (vs SCE)	0.1 M NaOH	22
PB-RGO	27.78	~~	7.94	−0.05 (vs Ag/AgCl)	0.05 M PB	36
Fe-doped $NiCo_2O_4$	3055.7	0.2~3100	0.19	0.5 (vs SCE)	0.1 M NaOH	37
Co–Ni(Fe)-MOF/PPy	1805	2~3000	1.13	0.6 (vs Hg/HgO)	0.1 M NaOH	38
Ni-MOF@Ni-HHTP-5	2124.9	0.5~2665.5	0.02	0.6 (vs Ag/AgCl)	0.1 M NaOH	39
Cu@Ni CSNPs/CNCs/NF	6905	1~1630	0.03	0.65 (vs Hg/HgO)	0.1 M NaOH	40
HTPBA/NF-12	**21410, 3749**	**2~450, 450~1250**	**0.089**	**0.5 (vs Ag/AgCl)**	**0.1 M NaOH**	**This work**

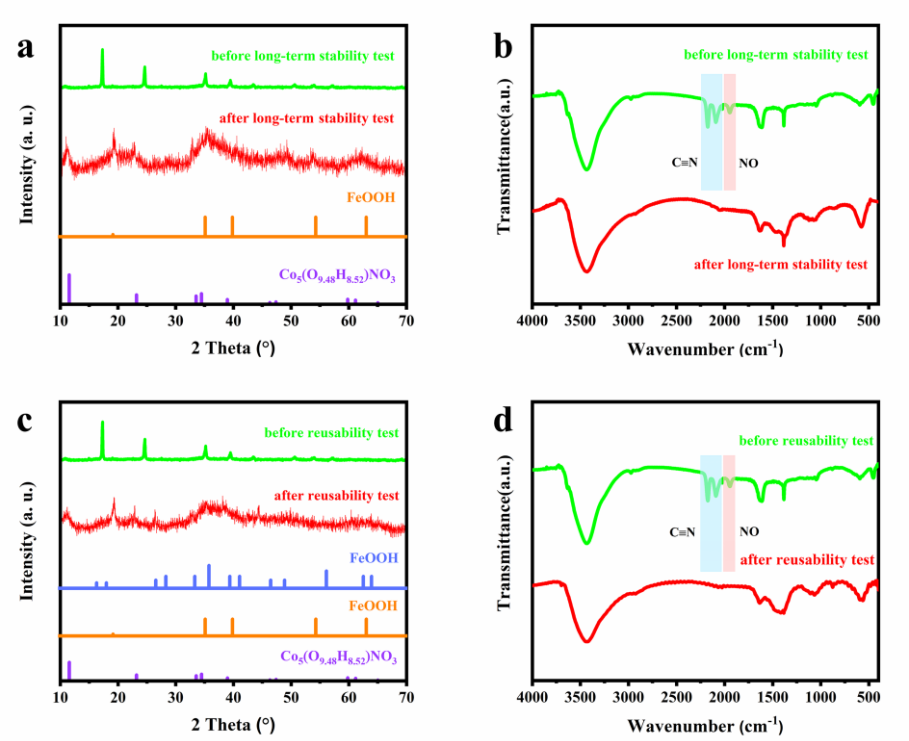

Fig. S6 The (a, c) XRD and (b, d) FT-IR pattern of HTPBA/NF-12 after long-term stability and reusability test.

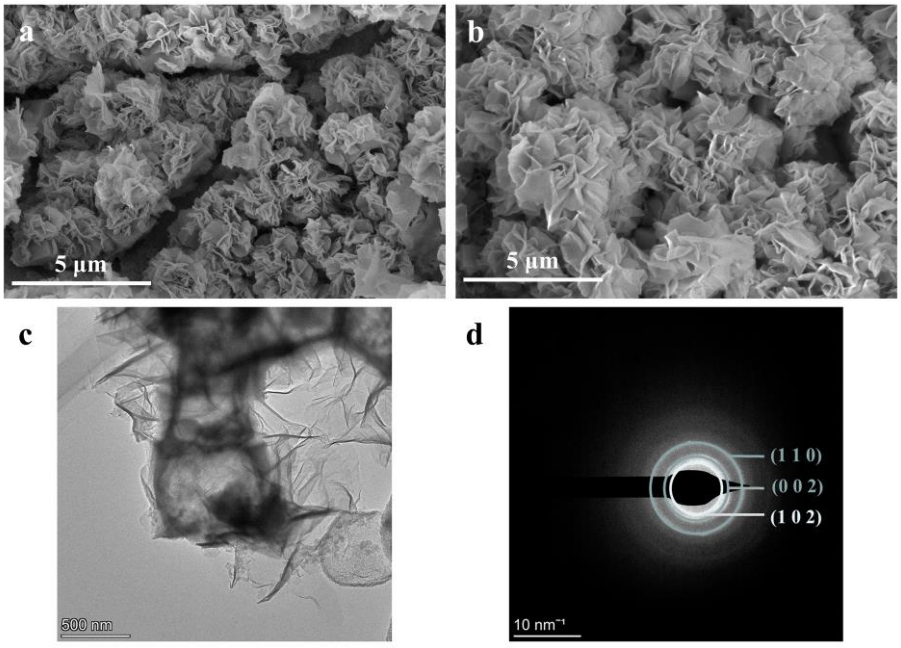

Fig. S7 SEM image of HTPBA/NF-12 after (a) long-term stability and (b) reusability test; (c) TEM image and (d) SAED pattern of HTPBA/NF-12 after long-term stability.

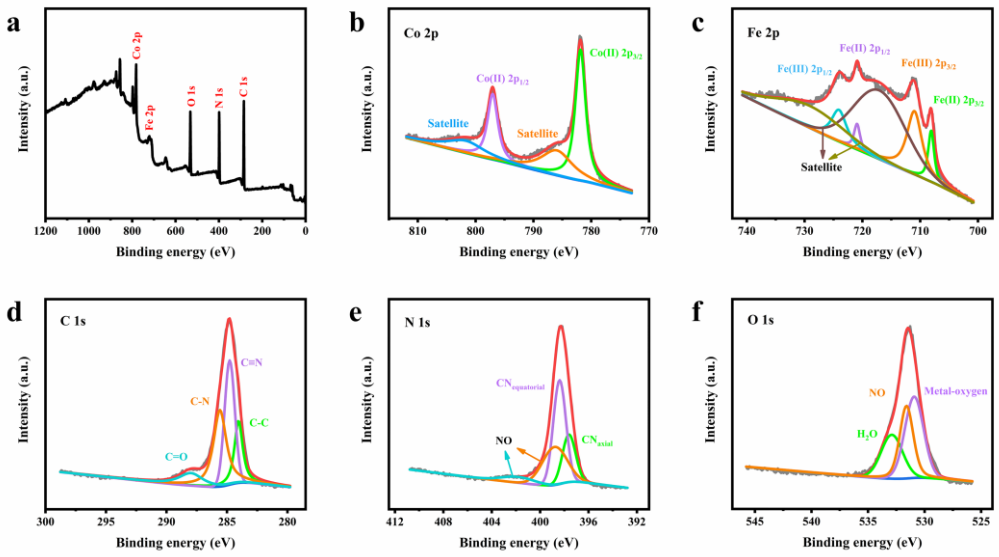

Fig. S8 (a) The XPS survey spectra of HTPBA/NF-12; High-resolution XPS spectra for the (b) Co 2p, (c) Fe 2p, (d) C 1s, (e) N 1s and (f) O 1s of HTPBA/NF-12.

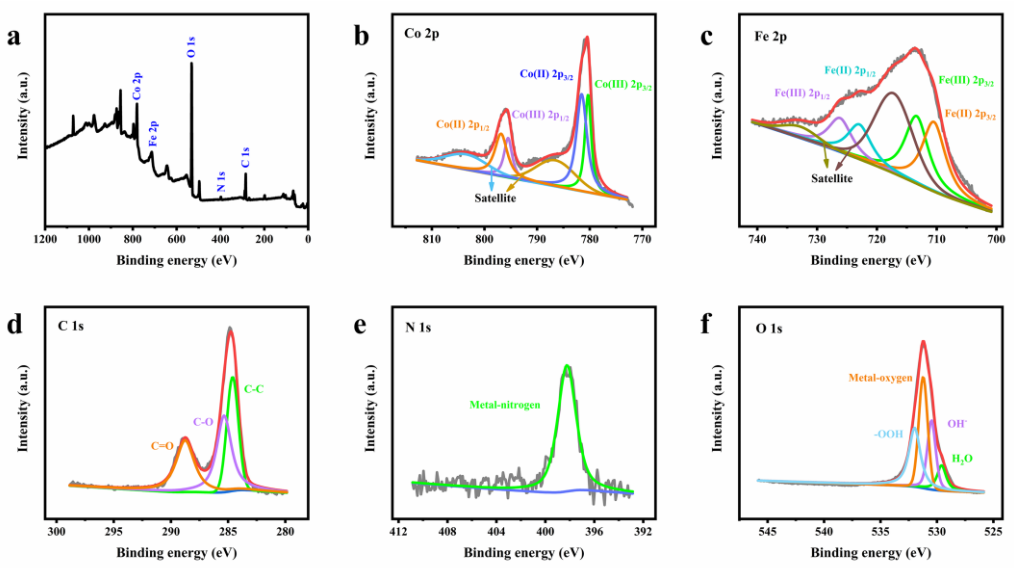

Fig. S9 (a) The XPS survey spectra of HTPBA/NF-12 after long-term stability test; High-resolution XPS spectra for the (b) Co 2p, (c) Fe 2p, (d) C 1s, (e) N 1s and (f) O 1s of HTPBA/NF-12 after long-term stability test.

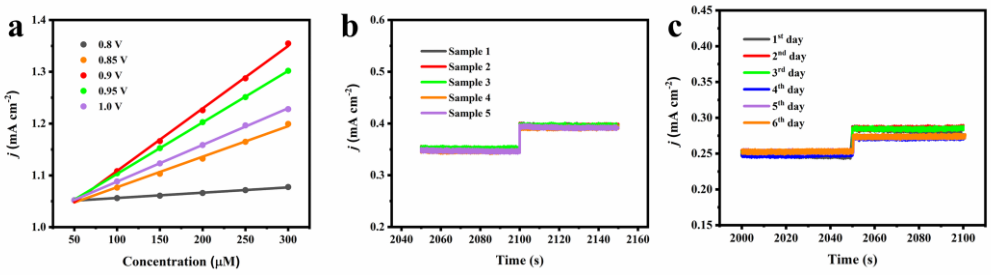

Fig. S10 (a) Optimization of detection potential; The (b) reproducibility and (c) reusability test of HTPBA/NF-12 by repeatedly measure current response to 40 μM $NaNO_2$.

Table S3. The comparison of sensing performance toward $NaNO_2$ between this work and other previous works.

Electrode	Sensitivity, ($\mu A\ mM^{-1}cm^{-2}$)	Linear Range, (μM)	LOD, (μM)	Working potential, (V)	Electrolyte (pH)	Ref.
PANI-MnO_2 nanocomposite	225	19.98~732.17	1.08	0.85 (vs SCE)	0.1 M PBS (5.0)	55
$NiCo_2O_4$/GCE	1030	10~300	1.04	0.75 (vs Ag/AgCl)	0.1 M PBS (7.0)	59
AgNC@NCS	~~	1.12~1400	0.38	~~	0.1 M PB (5.2)	62
$ZnLX_2$/SPCE	~~	2~500, 500~4838	0.78	0.85 (vs Ag/AgCl)	0.01 M PBS (4.4)	63
PPy/UiO-66/GCE	297.7	0.05~1055.5	0.037	1.05 (vs SCE)	0.1 M PBS (6.5)	64
$LaAlO_3$@GO/GCE	1132, 1176	0.01~1540.5	0.0041	0.9 (vs Ag/AgCl)	0.1 M PB (7.0)	65
Ni/MoS_2/GCE	72.47	5~800	2.48	~~	0.1 M PBS (4.0)	66
Near-spherical ZnO/GCE	785	0.6~220, 460~5500	0.39	1.05 (vs SCE)	0.1 M PBS (7.4)	67
GO-PANI-AuNPs/GCE	~~	0.5~240, 240~2580	0.17	0.9 (vs SCE)	0.1 M PBS (6.0)	68
HTPBA/NF-12	**1248, 705.8**	**5~1280, 1280~3380**	**0.38**	**0.9 (vs Ag/AgCl)**	**0.1 M PB (7.5)**	**This work**

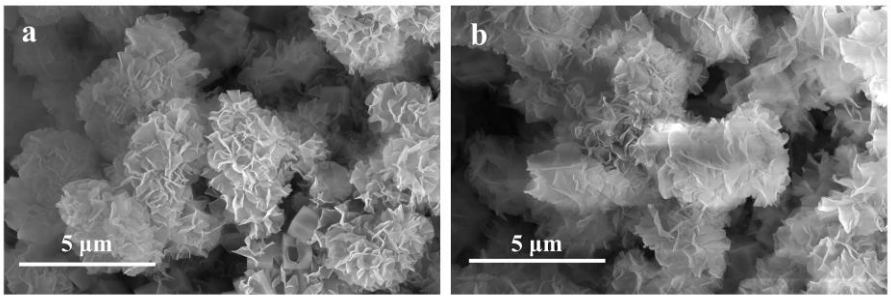

Fig. S11 The SEM image of HTPBA/NF-12 after (a) long-term stability and (b) reusability test.

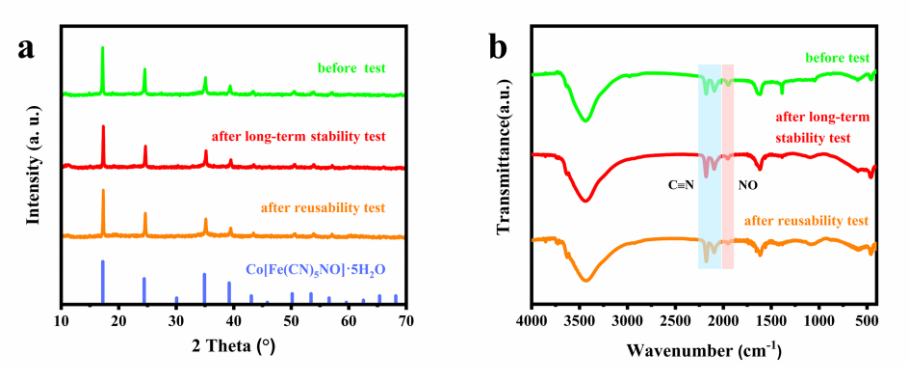

Fig. S12 The (a) XRD and (b) FT-IR pattern of HTPBA/NF-12 after long-term stability and reusability test.

Table S4. The Comparison of sensing performances between HTPBA/NF-12 and cubic CoFePBA towards glucose and $NaNO_2$ detection.

Detection target	Electrode	Sensitivity, ($\mu A\ mM^{-1}cm^{-2}$)	Linear Range, (μM)	LOD, (μM)
glucose	Cubic CoFePBA/NF	2644, 1331	10~480, 480~1280	0.38
	HTPBA/NF-12	**21410, 3749**	**2~450, 450~1250**	**0.089**
$NaNO_2$	Cubic CoFePBA/NF	458.4, 373.6	5~1530, 1530~3330	1.4
	HTPBA/NF-12	**1248, 705.8**	**5~1280, 1280~3380**	**0.38**

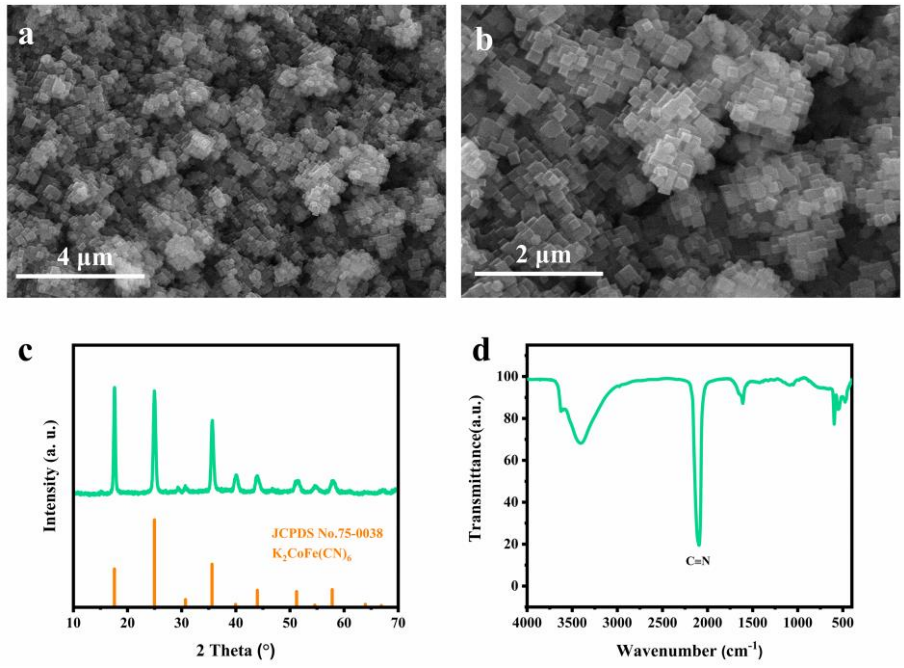

Fig. S13 (a-b) SEM image, (c) XRD and (d) FT-IR pattern of cubic CoFePBA/NF.

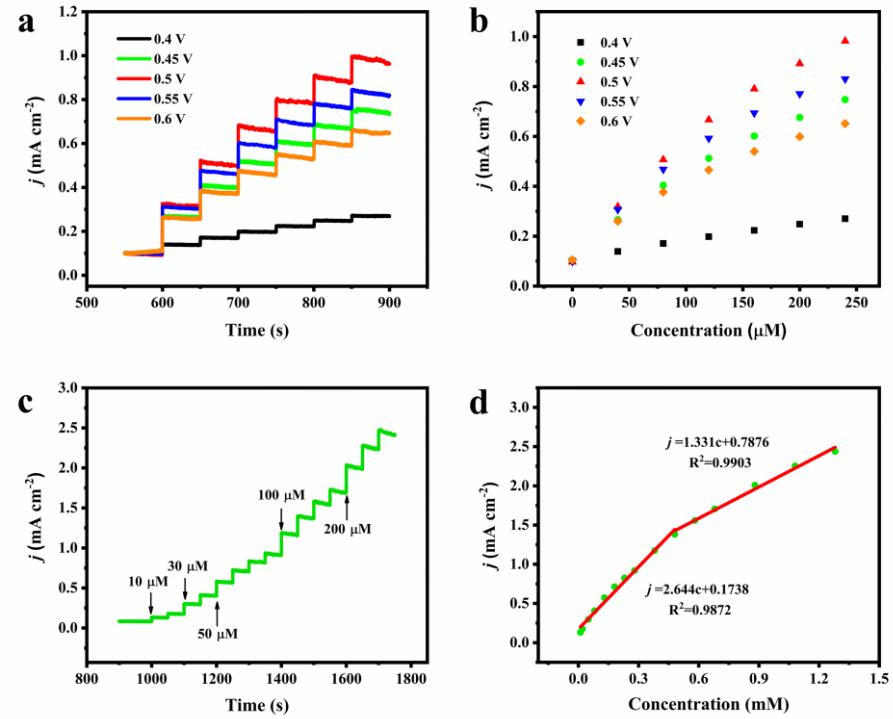

Fig. S14 (a-b) Potential optimization for cubic CoFePBA/NF towards glucose; (c-d)

Sensitivity test of cubic CoFePBA/NF at 0.5 V in 0.1 M NaOH.

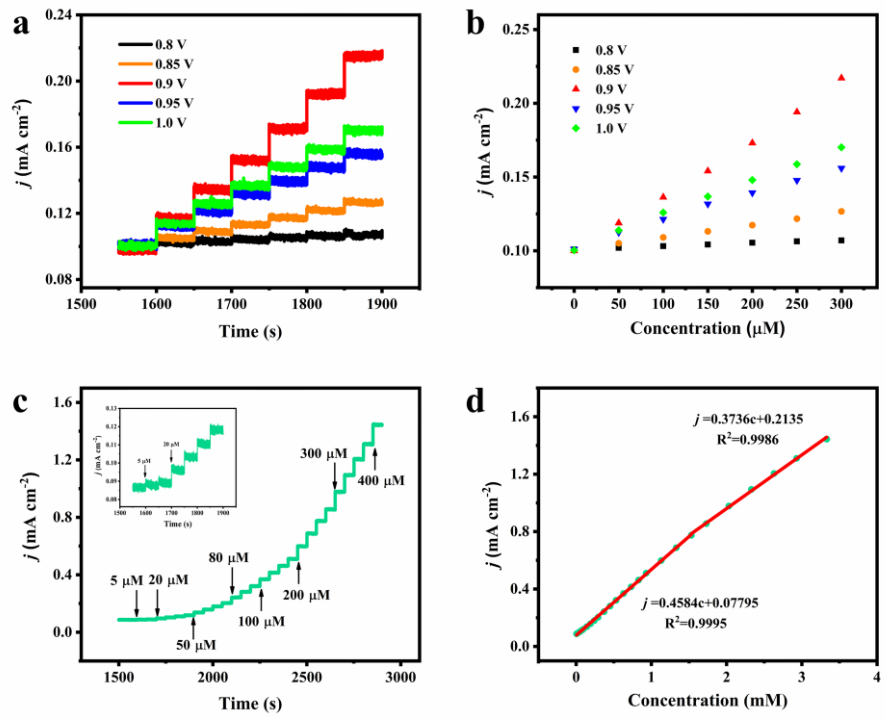

Fig. S15 (a) Chronoamperometric response of cubic CoFePBA/NF under different applied potential; (b) the plots of peak current density vs. $NaNO_2$ concentration; (c) Amperometric responses of cubic CoFePBA/NF injecting various concentration $NaNO_2$ in 0.1 M PB at 0.9 V (inset: the current response under a low $NaNO_2$ concentration); (d) Corresponding calibration curve.

Another CoFePBA material was synthesized based on similar synthetic process as HTPBA/NF-12, except that the same amount of potassium ferricyanide ($K_3[Fe(CN)_6]$ was used instead of sodium nitroprusside ($Na_4[Fe(CN)_5(NO)]$ in solution A. The reaction solution was maintained at 90 °C for 2 h. The obtained CoFePBA material was namely as cubic CoFePBA. SEM results as shown in Fig. S13a-b also demonstrate its cubic morphology with particle sizes of about 100-200 nm. Then, XRD and FT-IR as shown in Fig. S13c-d confirm its successful synthesis of CoFePBA material. As shown in Fig. S13c, all diffraction peaks in its XRD pattern match well with the characteristic peaks of $K_2CoFe(CN)_6$ (JCPDS 75-0038). In FT-IR

diagram, the peak at 2098 cm^{-1} can be attributed to the stretching vibration of C≡N, that is the characteristic peak of PBA material, suggesting the successful preparation of cubic CoFePBA on the surface of nickel foam.

As comparison, the sensing performances of cubic CoFePBA/NF towards glucose and nitrite were tested under the optimal test conditions. As shown in Fig. S14, its sensing sensitivity as glucose sensor was calculated to be 2644 and 1331 μA mM^{-1} cm^{-2} in the linear intervals of 10~480 and 480~1280 μM, respectively. The corresponding LOD was calculated to be 0.38 μM. As nitrite sensor as shown Fig. S15, its sensitivity toward low and high concentration of NO_2^- was calculated to be 458.4 (5~1530 μM) and 373.6 μA mM^{-1} cm^{-2} (1530~3330 μM), respectively, and the LOD was 1.4 μM.

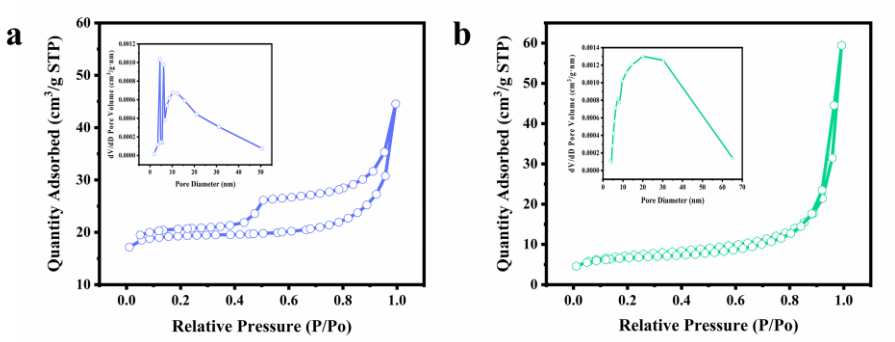

Fig. S16 N_2 adsorption-desorption isotherm at 77 K of (a) HTPBA/NF-12 and (b) cubic CoFePBA/NF (inset: the pore size distribution).